

BIO-INSPIRED AM STRUCTURE WITH CARBON FIBRE REINFORCEMENT

P. Jameekornkul*, A. Panesar*

* IDEA Lab, Department of Aeronautics, Imperial College London, UK

Abstract

This study presents a novel design approach that introduces the bouligand fibre arrangement in a honeycomb structure. This design is made possible by utilising AM technology which allows for the realisation of complex design whilst ensuring precise control for fibre placement. Reinforced honeycomb structures with varied incrementally twisted pitch angle of 0° , 1.25° , 5° and 15° were successfully fabricated and tested under out-of-plane compression. Among the tested angles, the honeycomb structure oriented at 1.25° exhibited higher peak load and higher specific energy absorption. Unlike the original untwisted honeycomb, the bio-inspired honeycomb showed no noticeable buckling or delamination at the mid-plane, which may be due the microcracking or resulting from a delay in crack propagation. However, the precise relationship between pitch angle and honeycomb properties requires further investigation across a wider range of pitch angle with more focus understanding the fracture propagation in fibre arrangement. Overall, the preliminary results indicate that the proposed bio-inspired AM design present a promising approach to enhance the properties of honeycombs and afford the flexibility to improve toughness and energy absorption capabilities.

Introduction

Bouligand structure

Over the course of many years, nature has evolved structures that possess remarkable characteristics. Bio-inspired structures have gained significant attention in recent years due to their remarkable energy absorption capabilities and their potential applications in areas such as damage mitigation. One of bio-inspired structure which was adapted in manufacturing the composite structure is Bouligand structure introduced by Bouligand in 1972 [1] or the helicoidal formation. The formation consisting of unidirectional fibrous layer orientating around the centre with a constant pitch angle (γ) throughout the stack of layers [2]. This type of structure arrangement could be found in natural microstructure and have been studied by researchers, for example, mantis shrimp [3], DNA structure, the cuticle of scorpion chela [4], palm leaf [5] [6], arthropod phylum [7] and bone minerals [7].

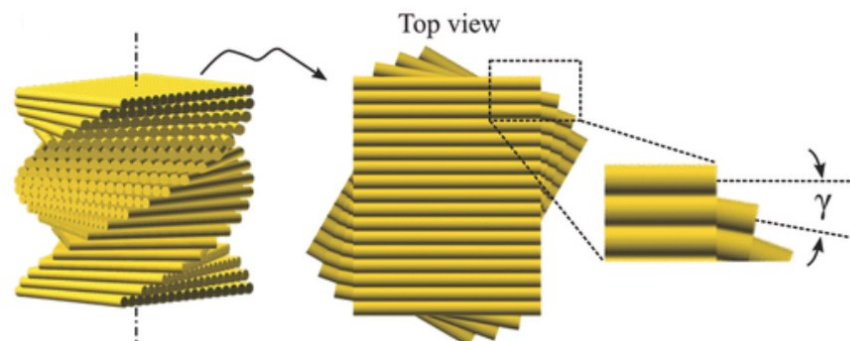


Figure 1: The schematic of helicoidal fibre structure where γ is a constant pitch angle. [8]

The helicoidal fibre structure has been shown to provide high interfacial strength, maximise transverse load resistance [13-14], delaying the fracture propagation, higher damage resistance compare to conventional cross ply [11], energy absorption ability, remarkable toughness and the impact strength [4] [12] [13]. These

features associated with the twisting of reinforcement fibre along with the stacking direction and therefore, force the crack to twist as they grow parallel to the fibre orientation [14]. Another feature of helicoidal structure is creating microcracks within the structure and increase in the surface crack area which responsible for more energy able to be absorbed before the catastrophic failure [14]. Apart from experimental investigation, theoretical models were proposed for optimal pitch angle [15] and crack growth behaviour [14]. So far, most helicoidal structure studies focused on a laminate lay-up which limited the geometric freedom. Therefore, this study aims to utilise the capabilities of AM technique to further control the helicoidal inspired fibre structure.

Failure mechanism in fibre composite

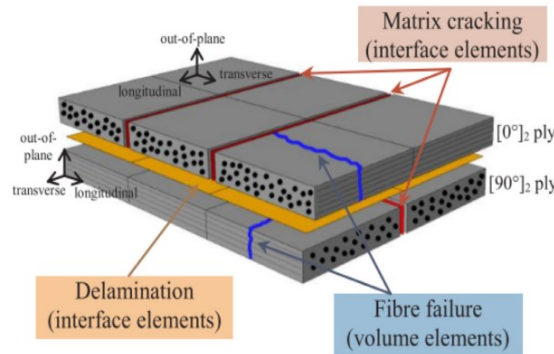


Figure 2: Major failure modes observed for the fibre reinforced composite [16]

Major failure mechanisms occurred within composite with fibre reinforcement are delamination, propagation of the matrix cracking and fibre failure [17], [18] (Figure 2). It can be summarised from a review [16] of composite structure that different failure modes were observed in varied mode of fracture classification (Mode I, II and III) and different composite shapes e.g., tubes, sections, and cellular structures resulting in changing of the crashworthiness performance.

While AM technology has not been commonly used and studied for composite thin-wall tube, the filament winding and lay-up technique have known for mass production of carbon fibre-reinforced polymer (CFRP) tubes which normally have reinforcement layers at the outer skin. Ma et al. [18] conducted an axial crushing on a hybrid composite tubes suggested that the CFRP circular tube absorbed energy through fibre fracture, matrix failure and interlayer fracture [19] which demonstrated through the outer layer of reinforcement rolled out while the inner layer is bent and fractured [18] [20]. The study confirmed the failure mechanism and progressive collapse behaviour are the key to crash efficiently of thin-walled composite tube. Thus, here, we will examine the failure mechanisms that occur in our modified structure to understand crashworthiness performance at the root causes.

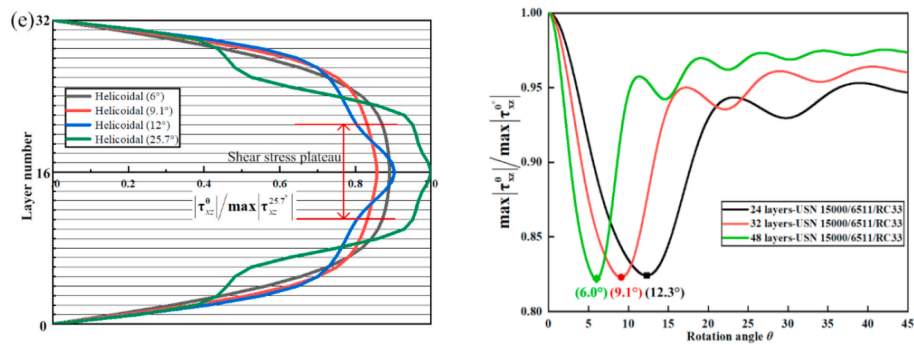


Figure 3: a.) Interlaminar shear stress distribution predicted in [15] varying the pitch angle
b.) the optimal rotation angle for different total number of laminae [15]

Aims

Honeycomb characterised by their hexagonal cell structure which capable of optimising the space filling, are widely used in sandwich structures to provide superior strength and stiffness while maintaining a lightweight profile. In this study, our design involves a modified honeycomb structure with a helicoidal fibre arrangement. The objective is to leverage the advantages offered by bio-inspired structures, specifically focusing on enhancing energy absorption capability and improving fracture toughness. Our aim is to explore novel approaches for achieving controlled crack propagation by utilising the continuous additive manufacturing (AM) technique, which enables complex part design and tailorable fibre placement.

Therefore, we will investigate the compression properties of this bio-inspired honeycomb structures, focusing on their potential for energy absorption applications. experiments will be conducted to assess the feasibility and effectiveness of the proposed design concept. Specifically, the mechanical performance and energy dissipation capabilities of a thin-walled tube with a helicoidal-honeycomb profile will be evaluated. These experiments will provide insights into the performance characteristics of the bio-inspired structure and its potential for extending the concept to further applications.

Methodology

Design process

A single honeycomb structure was designed using the Solidworks software, and its dimensions are presented in Figure 4a. The structure consists of 48 layers and has a height of 17.7 mm. Figure 4a demonstrates the twisting of the honeycomb by shifting the XY coordinates based on the pitch angle θ around the fixed centre point (a, b). The pitch angle was varied at intervals of 1.25° , 5° , and 15° , resulting in 1, 4, and 12 full rotations within the sample, respectively. Figure 4b is an example of travel path of the printer nozzle when the honeycomb was shifted using a 15° pitch angle.

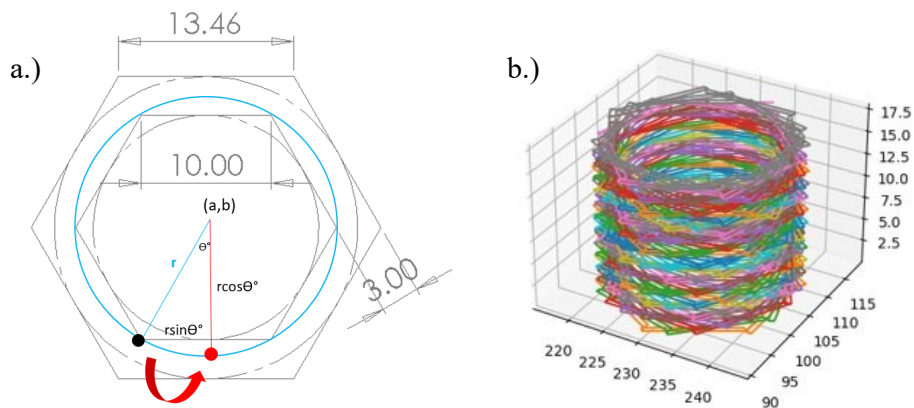


Figure 4: a.) Dimension of honeycomb (top view)
b.) trajectory of nozzle for sample with 48 layers and 15 degrees pitch angle

Manufacturing process

The material extrusion technique is chosen for the fabricating of the samples using Anisoprint, a printer with capability of co-extruding the fibre reinforcement and matrix. The G-CODE, responsible for controlling the nozzle's path and the amount of material extrusion, was modified to achieve the desired helicoidal fibre arrangement in the printed structure.

To ensure the structural integrity, the limitation of printing process was determined. The minimum length of the inner side of the honeycomb should at least 7.5 mm to avoid the fibre curvature and fibre twisting. In addition, the preliminary printing test was conducted to determine the appropriate volume fraction between the carbon fibre reinforcement and matrix for the printing. The volume fraction plays a significant role in the properties of the printed specimen, as the quality of bonding between the matrix and the fibres directly depends on this parameter.

During the manufacture, the model dimensions, volume fraction and the amount of material extruded were kept unchanged. The matrix material used was PETG, while carbon fibre was employed as the continuous fibre reinforcement (refer to Table 1 for combined material properties). To maintain continuity, the fibre reinforcement was only cut once at the end of each layer. The feed rate and travel speed were set to the default values provided by the Aura slicer software. The nozzle temperature and build plate temperature were consistently maintained at 245°C and 60°C, respectively.

Table 1: Carbon fibre and matrix properties [21]

Materials	Compressive Strength (MPa)	Compressive Modulus (GPa)
CCF-1.5K-PETG	237.4 ± 4.2	49.0±2.4



Figure 5: Printed specimen (15°, 5°, 1.25° pitch angle from right to left)

Figure 5 displays the printed specimens with varying pitch angles. It is important to mention that the default slicer settings resulted in an excess of PETG material at the start of each layer, which could be removed through post-processing. However, to maintain the integrity of the bonding properties, post-processing was not performed. To ensure fairness in the experiment, the weight of each specimen was measured, and it was confirmed that an equal amount of excess plastic was present at each layer in all specimens and will not impact the experimental results.

Experiment

The out-of-plane compression test was carried out using the 50kN Instron 5969 machine, with a constant displacement rate of 1mm/min. The video camera was used to record the experiment in order to observe the failure mechanism along with time mark. For each sample, three specimens were tested. Additionally, a video camera was used to record the test, facilitating fracture investigation. Following the compression test, the failed specimens will be examined using a scanning electron microscope (SEM), with a focus on observing crack initiation and propagation. It is important to note that the experiment was conducted within 72 hours after the fabrication process to minimize the potential impact of moisture absorption in PETG.

In order to further the understanding of compressive behaviour, the specific energy absorption (SEA) will be calculated from Equation (1).

$$SEA = \frac{E}{m} \quad \text{(Equation 1)}$$

where E is the total energy absorbed which equal to area under force-displacement curve following equation 2 and m is mass of material (kg) which is an average weight of all printed specimens (0.39 g).

$$E = \int_0^{d_{max}} F ds \quad (\text{Equation 2})$$

where d_{max} is the maximum displacement achievable by all specimens. To distinguish between the elastic and plastic phase, the yield strength determined by the stress value which corresponding to the 0.2% offset strain. The highest stress value of the stress-strain curve before reaching the densification phase at the end will be defined as the ultimate strength.

Results and Discussions

Stress-strain curve and pitch angle effect

In Figure 6, the stress-strain plot demonstrates a similar pattern of ductile materials behaviour across the range of pitch angle. The specific energy absorbed, ultimate strength and yield strength are calculated and illustrated in according to pitch angle in Figure 7. The experiment showed that the orientation of reinforcement in each layer affects both peak force and specific energy absorbed (Figure 7). The rotation angle of 1.25° has shown the highest energy absorbed by achieving the highest ultimate strength and the smallest stress drop level, indicating a less catastrophic shear failure at the end. While the rotation angle of 15° showed higher peak load and modulus compared to the normal honeycomb but experienced a significant drop in stress afterwards.

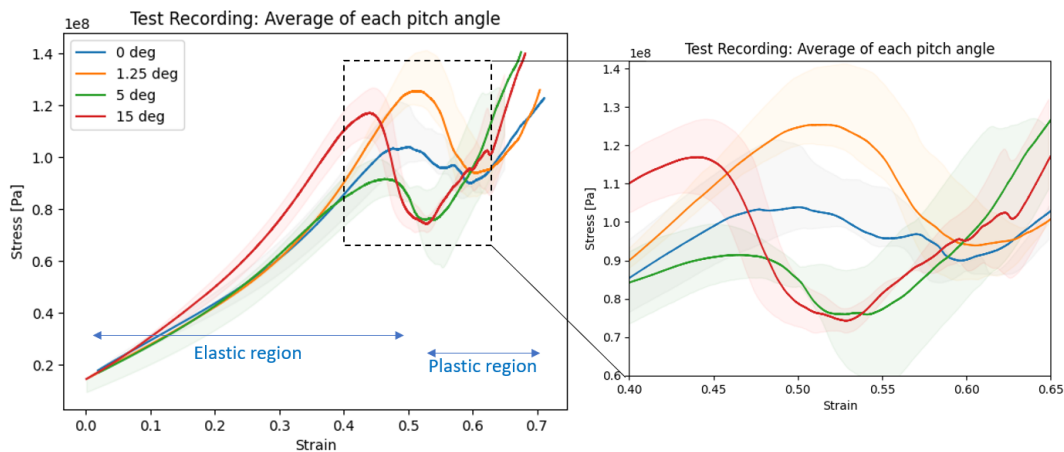


Figure 6: Stress-Strain plot for compression experiment varying pitch angle.

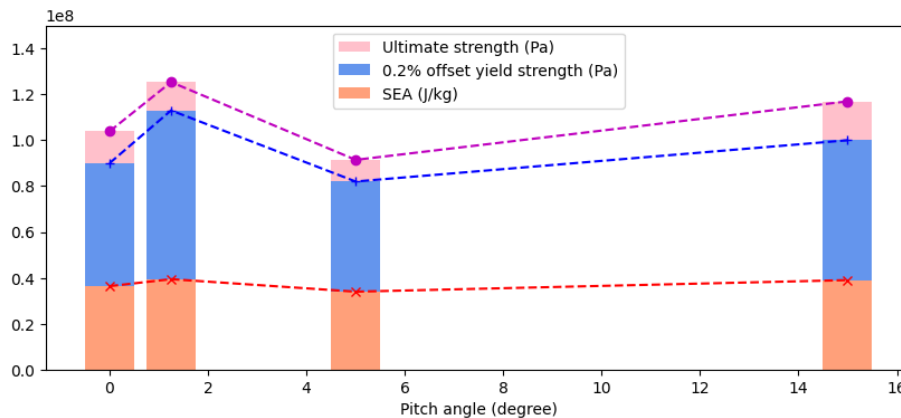


Figure 7: Properties of varying pitch angle calculated from displacement-load curve.

Both specimen of 5° and 15° orientations reached peak strength at lower strain than the normal honeycomb and leads to a lower stress before entering densification phase. Although no clear trend was observed between properties and the pitch angle, our most successful samples, specifically those with a 1.25° rotation angle, align with the natural bioligand structure observed at approximately 1.6° and supported by studies [22] [23] which indicate that indicate superior performance with smaller pitch angles under their conditions.

The potential cause of performance fluctuation at different pitch angle is suspected to be attributed to the interlaminar shear behaviour. This interlaminar shear distribution was affected by the fibre stacking orientation, ply thickness and total number of stacking ply [15]. The prediction model proposed by [15] showed that plateau stress was not linearly proportional to pitch angle (Figure 3b and c). In addition, [23] suspected that the fluctuation could be affected by the fibre intersection points changed by pitch angle causing the stress and fracture to propagate differently.

It is important to note that this study introduces the honeycomb structure alongside with AM technique, which potentially contributes to the observed fluctuations due to manufacturing and complex design effect causing inconsistency fibre spacing and layer thickness [14]. In addition, the number of full rotations back to original first layer should be taken in account. Therefore, a broader range of pitch angle and an effect of rotation rounds was planned to be investigated further.

Failure modes

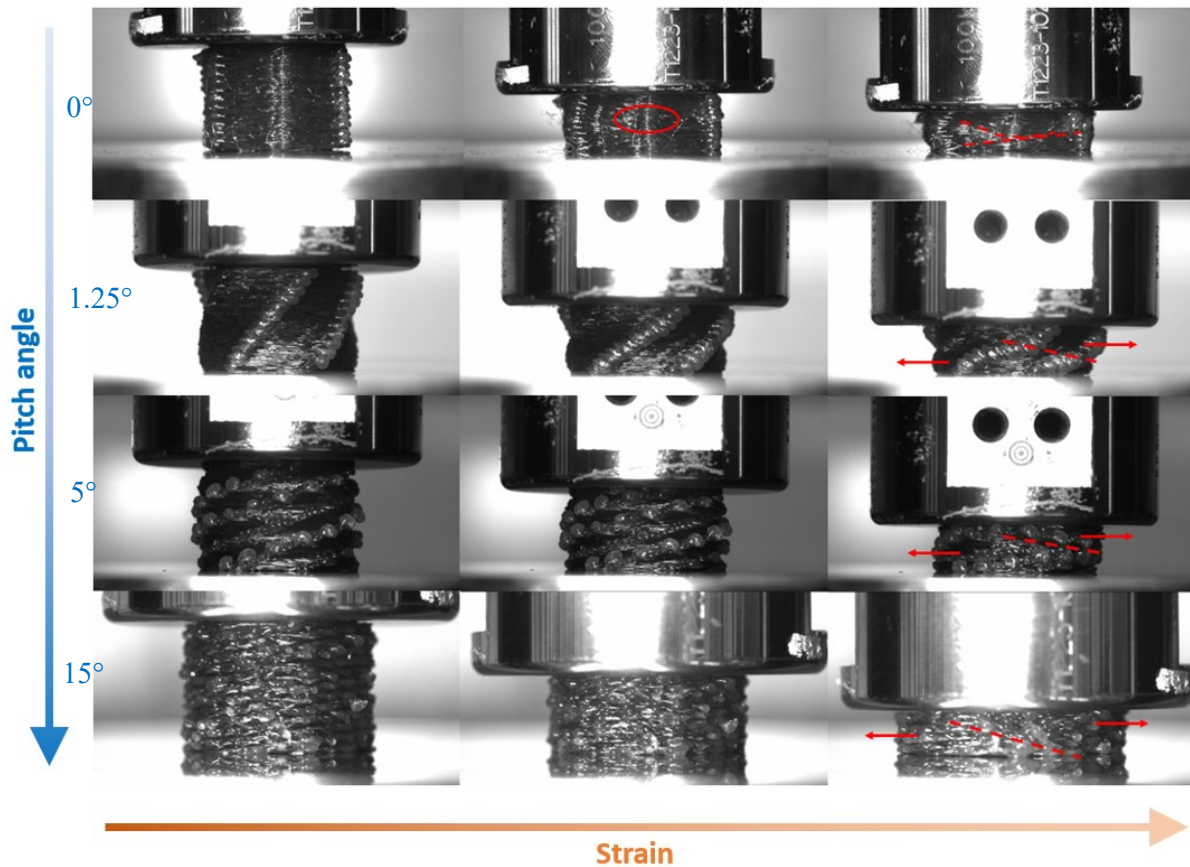


Figure 8: The failure behaviour during the quasi-static compression test captured by a video camera (Pitch angle 0° , 1.25° , 5° , 15° from top to bottom).

Figure 8 and Figure 9a show the sign of buckling and delamination in the mid-plane of the print direction of the zero-degree honeycomb. This observation aligns with the findings of Zhang and Ashby [24] which expected the honeycomb to buckle elastically. However, the samples with positive pitch angle did not clearly show the delamination or buckling, this could be due to the microcracking occurring inside of the structure, or the progressive collapse at slower rate, or the buckling was delayed and cannot be captured by video camera. Further in-situ measurement where the load will be stopped for observation could be conducted.

Apart from general trend of stress-strain curve, all specimens shown similar shear failure (see last column of Figure 8) starting from the mid-plane progressing towards the bottom layer (Figure 9b and c) after the upper yield stress was reached. The shear failure can be clearly seen in SEM images that both fibre and matrix shown catastrophic failure in the said direction. This shear catastrophic failure then causes the delamination between interfaces before entering the densification phase at the end.

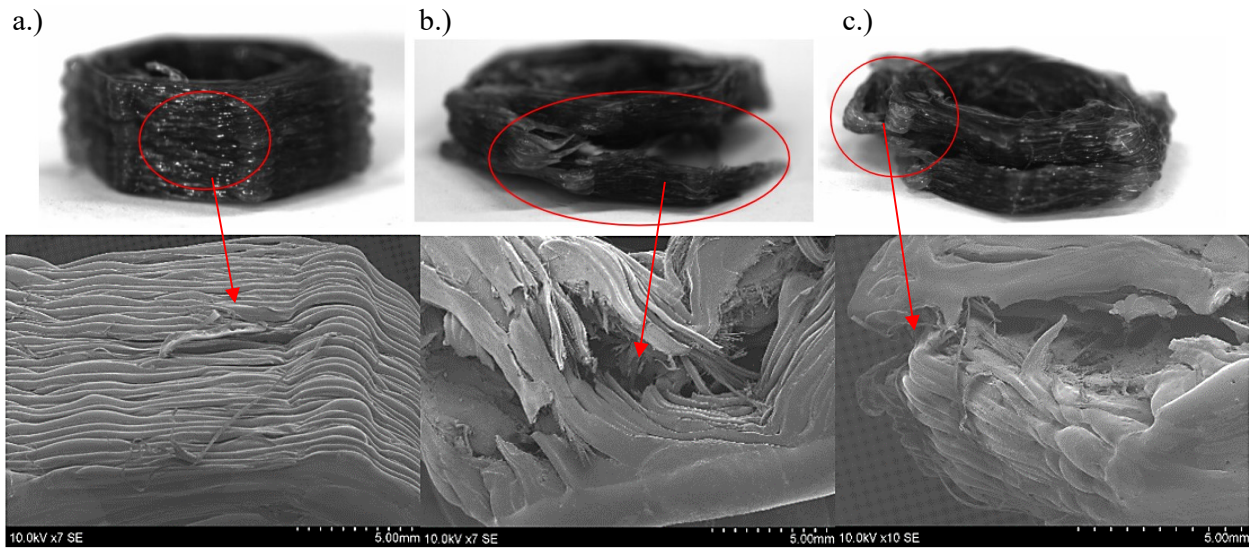


Figure 9: Failed specimens (first row) and SEM images (second row) show a.) buckling in mid-plane of original honeycomb b-c.) Shear failure at the bottom layer.

Conclusion

The preliminary results obtained from the compression test revealed a consistent trend in the stress-strain curve. However, the ultimate strength and the point at which stress dropped due to shear failure varied with different pitch angles. The orientation and alignment of the fibres were influenced by the pitch angle, leading to potential differences in crack propagation rates and the presence of invisible microcracks. Consequently, the mechanical properties exhibited fluctuations depending on the pitch angle, requiring further investigation to establish a prediction model. A broader range of pitch angles should be explored in future studies, and the compression test could be paused at different phases to gain a deeper understanding of fracture mechanics.

In terms of quality inspection, shear failure at both fibre and matrix was observed in all specimens, while only the conventional honeycomb showed signs of buckling and crack propagation. Notably, the investigation revealed that the honeycomb with a pitch angle of 1.25° exhibited superior energy absorption capabilities, aligning well with previous literature and numerical prediction models. This bio-inspired honeycomb design holds promise for further modifications to incorporate multiple cellular structures in sandwich applications, enhancing its potential for adoption across various industries.

Reference

- [1] Y. Bouligand, 'Twisted fibrous arrangements in biological materials and cholesteric mesophases', *Tissue Cell*, vol. 4, no. 2, pp. 189–217, 1972, doi: 10.1016/s0040-8166(72)80042-9.
- [2] I. Greenfeld, I. Kellersztein, and H. D. Wagner, 'Nested helicoids in biological microstructures', *Nat. Commun.*, vol. 11, no. 1, Art. no. 1, Jan. 2020, doi: 10.1038/s41467-019-13978-6.
- [3] Q. Han *et al.*, 'Impact resistant basalt fiber-reinforced aluminum laminate with Janus helical structures inspired by lobster and mantis shrimp', *Compos. Struct.*, vol. 291, p. 115551, Jul. 2022, doi: 10.1016/j.compstruct.2022.115551.
- [4] D. Raabe, C. Sachs, and P. Romano, 'The crustacean exoskeleton as an example of a structurally and mechanically graded biological nanocomposite material', *Acta Mater.*, vol. 53, no. 15, pp. 4281–4292, Sep. 2005, doi: 10.1016/j.actamat.2005.05.027.
- [5] E. Mahdi, D. Ochoa, A. Vaziri, and E. Eltai, 'Energy absorption capability of date palm leaf fiber reinforced epoxy composites rectangular tubes', *Compos. Struct.*, vol. 224, p. 111004, Sep. 2019, doi: 10.1016/j.compstruct.2019.111004.
- [6] E. Mahdi, A. S. M. Hamouda, and A. C. Sen, 'Quasi-static crushing behaviour of hybrid and non-hybrid natural fibre composite solid cones', *Compos. Struct.*, vol. 66, no. 1, pp. 647–663, Oct. 2004, doi: 10.1016/j.compstruct.2004.06.001.
- [7] L. Cheng, A. Thomas, J. L. Glancey, and A. M. Karlsson, 'Mechanical behavior of bio-inspired laminated composites', *Compos. Part Appl. Sci. Manuf.*, vol. 42, no. 2, pp. 211–220, Feb. 2011, doi: 10.1016/j.compositesa.2010.11.009.
- [8] A. Zaheri *et al.*, 'Revealing the Mechanics of Helicoidal Composites through Additive Manufacturing and Beetle Developmental Stage Analysis', *Adv. Funct. Mater.*, vol. 28, Aug. 2018, doi: 10.1002/adfm.201803073.
- [9] J. S. Shang, N. H. H. Ngern, and V. B. C. Tan, 'Crustacean-inspired helicoidal laminates', *Compos. Sci. Technol.*, vol. 128, pp. 222–232, May 2016, doi: 10.1016/j.compscitech.2016.04.007.
- [10] T. Apichattrabrut and K. Ravi-Chandar, 'Helicoidal Composites', *Mech. Adv. Mater. Struct.*, vol. 13, no. 1, pp. 61–76, Jan. 2006, doi: 10.1080/15376490500343808.
- [11] L. Cheng, L. Wang, and A. M. Karlsson, 'Mechanics-based analysis of selected features of the exoskeletal microstructure of *Popillia japonica*', *J. Mater. Res.*, vol. 24, no. 11, pp. 3253–3267, Nov. 2009, doi: 10.1557/jmr.2009.0409.
- [12] J. L. Liu, H. P. Lee, and V. B. C. Tan, 'Effects of inter-ply angles on the failure mechanisms in bioinspired helicoidal laminates', *Compos. Sci. Technol.*, vol. 165, pp. 282–289, Sep. 2018, doi: 10.1016/j.compscitech.2018.07.017.
- [13] H. Jiang, Y. Ren, Z. Liu, S. Zhang, and Z. Lin, 'Low-velocity impact resistance behaviors of bio-inspired helicoidal composite laminates with non-linear rotation angle based layups', *Compos. Struct.*, vol. 214, pp. 463–475, Apr. 2019, doi: 10.1016/j.compstruct.2019.02.034.
- [14] N. Suksangpanya, N. A. Yaraghi, D. Kisailus, and P. Zavattieri, 'Twisting cracks in Bouligand structures', *J. Mech. Behav. Biomed. Mater.*, vol. 76, pp. 38–57, Dec. 2017, doi: 10.1016/j.jmbbm.2017.06.010.
- [15] W. Ouyang, B. Gong, H. Wang, F. Scarpa, B. Su, and H.-X. Peng, 'Identifying optimal rotating pitch angles in composites with Bouligand structure', *Compos. Commun.*, vol. 23, p. 100602, Feb. 2021, doi: 10.1016/j.coco.2020.100602.
- [16] C. W. Isaac and C. Ezekwem, 'A review of the crashworthiness performance of energy absorbing composite structure within the context of materials, manufacturing and maintenance for sustainability', *Compos. Struct.*, vol. 257, p. 113081, Feb. 2021, doi: 10.1016/j.compstruct.2020.113081.
- [17] N. Dubary, C. Bouvet, S. Rivallant, and L. Ratsifandrihana, 'Damage tolerance of an impacted composite laminate', *Compos. Struct.*, vol. 206, pp. 261–271, Dec. 2018, doi: 10.1016/j.compstruct.2018.08.045.
- [18] Q. Ma, R. Rejab, I. Mat Sahat, S. Hassan, and N. Manoj Kumar, 'Effect of winding angle on the quasi-static crushing behaviour of thin-walled carbon fibre-reinforced polymer tubes', *Polym. Polym. Compos.*, vol. 28, Oct. 2019, doi: 10.1177/0967391119887571.

- [19] R. Jiang *et al.*, 'Energy Absorption Characteristics of a CFRP-Al Hybrid Thin-Walled Circular Tube under Axial Crushing', *Aerospace*, vol. 8, no. 10, Art. no. 10, Oct. 2021, doi: 10.3390/aerospace8100279.
- [20] A. Farokhi Nejad, S. S. R. Koloor, M. L. H. Arifin, A. Shafiei, S. A. Hassan, and M. Y. Yahya, 'Crashworthiness Assessment of Carbon/Glass Epoxy Hybrid Composite Tubes Subjected to Axial Loads', *Polymers*, vol. 14, no. 19, p. 4083, Sep. 2022, doi: 10.3390/polym14194083.
- [21] 'CFC PETG', *Anisoprint*. <https://anisoprint.com/cfc-petg/> (accessed Jun. 28, 2023).
- [22] L. Mencattelli and S. T. Pinho, 'Realising bio-inspired impact damage-tolerant thin-ply CFRP Bouligand structures via promoting diffused sub-critical helicoidal damage', *Compos. Sci. Technol.*, vol. 182, p. 107684, Sep. 2019, doi: 10.1016/j.compscitech.2019.107684.
- [23] I. M. Van Meerbeek, J. M. Lenhardt, W. Small, T. M. Bryson, E. B. Duoss, and T. H. Weisgraber, 'Compressive properties of silicone Bouligand structures', *MRS Bull.*, vol. 48, no. 4, pp. 325–331, Apr. 2023, doi: 10.1557/s43577-022-00398-z.
- [24] J. Zhang and M. F. Ashby, 'The out-of-plane properties of honeycombs', *Int. J. Mech. Sci.*, vol. 34, no. 6, pp. 475–489, Jun. 1992, doi: 10.1016/0020-7403(92)90013-7.